Microsecond-to-Millisecond Conformational Dynamics Demarcate the GluR2 Glutamate Receptor Bound to Agonists Glutamate, Quisqualate, and AMPA†

Elizabeth R. Valentine and Arthur G. Palmer, III*

Department of Biochemistry and Molecular Biophysics, Columbia University, 630 West 168th Street, New York, New York 10032

Received September 17, 2004; Revised Manuscript Received December 17, 2004

ABSTRACT: Chemical shift changes and internal motions on microsecond-to-millisecond time scales of the S1S2 ligand-binding domain of the GluR2 ionotropic glutamate receptor have been studied by NMR spectroscopy in the presence of the agonists glutamic acid (glutamate), quisqualic acid (quisqualate), and α-amino-3-hydroxy-5-methyl-4-isoxazole propionic acid (AMPA). Although the crystal structures of the three agonist-bound forms of GluR2 S1S2 ligand-binding domain are very similar, chemical shift changes imply that AMPA-bound GluR2 S1S2 is conformationally distinct from glutamate- and quisqualate-bound forms of GluR2 S1S2. NMR spin relaxation measurements for backbone amide ^{15}N nuclei reveal that GluR2 S1S2 exhibits reduced chemical exchange line broadening, resulting from microsecond-to-millisecond conformational dynamics, in AMPA-bound compared to glutamate- and quisqualate-bound states. The largest changes in line broadening are observed for two regions of GluR2 S1S2: Val683 and the segment around Lys716-Cys718. The differences in binding affinity of these agonists do not explain the differences in microsecond-to-millisecond conformational dynamics because quisqualate and AMPA bind with similar affinities that are 10-fold greater than the affinity of glutamate. Differences in conformational mobility may reflect differences in the binding mode of AMPA in the GluR2 S1S2 active site compared to the other two ligands. The sites of conformational mobility in GluR2 S1S2 imply that subtle differences exist between the agonists glutamate, quisqualate, and AMPA in modulating glutamate receptor function.

Members of the ionotropic glutamate receptor (iGluR)[1] family mediate many of the excitatory responses in the central nervous system of higher eukaryotes and have been implicated in memory, learning, and various neurodegenerative diseases (*1*). The family is divided into three subcategories based on pharmacological properties and amino acid sequence similarity: the α-amino-3-hydroxy-5-methyl-4-isoxazole propionic acid (AMPA) receptors, GluR1−GluR4 (also known as GluRA−GluRD); kainate receptors, GluR5−7 and KA1−2; and *N*-methyl-D-aspartate (NMDA) receptors, NMDAR1 and NMDAR2a-NMDAR2d (*1*). Functional ionotropic glutamate receptors are tetrameric assemblies of the same protomer subtype that form a dimer of dimers (*2*−*7*). Each protomer consists of an N-terminal domain, a ligand-binding domain, three transmembrane domains, a re-entrant pore loop, and a C-terminal domain.

The ligand-binding domain (S1S2) of iGluR's is formed from two conserved amino acid sequence segments, denoted S1 and S2, with homology to bacterial periplasmic ligand-binding proteins (*1*). Ligand binding by the S1S2 domain has been investigated extensively in the absence of the other domains and membrane by using soluble protein constructs consisting of the S1 and S2 sequences joined by a hydrophilic linker peptide (*8*, *9*). Glutamic acid (glutamate), quisqualic acid (quisqualate), AMPA, and other ligands bind to these S1S2 constructs with affinities similar to those of their binding to intact transmembrane receptors (*8*, *9*). Such soluble S1S2 constructs also have proven useful in a variety of biophysical studies, including X-ray crystallography and NMR spectroscopy (*4*, *10*−*17*).

X-ray crystal structures of an optimized ligand-binding domain construct, named S1S2J (*4*), of GluR2 have been solved in the apo form and in complexes with a variety of agonists, partial agonists, and antagonists. Figure 1 shows a Cα chain trace of the soluble S1S2J ligand-binding domain bound to glutamate in the context of the putative intact GluR2 receptor. The overall structure of S1S2J consists of two structural domains: domain 1 is composed mostly of amino acid residues from S1, and domain 2 is composed mostly of amino acid residues from S2. Ligands bind in a cleft between the two domains, and the degree of closure between the two domains has been shown to be proportional to the efficacy of the specific ligand; i.e., agonists induce a greater degree of closure than antagonists (*4*).

X-ray crystal structures of GluR2 S1S2 complexed with the agonists glutamate, quisqualate, and AMPA are almost completely superposable and exhibit similar degrees of domain closure (*4*, *15*). Despite these similarities, as shown in Figure 2, AMPA interacts differently with active-site

† E.R.V. acknowledges support from a National Science Foundation Graduate Research Fellowship. A.G.P. acknowledges support from National Institutes of Health Grant GM59273. The cryoprobe accessory for the Bruker DRX600 NMR spectrometer was purchased with NIH Grant RR16785. A.G.P. is a member of the New York Structural Biology Center supported by NIH Grant GM66254.

* To whom correspondence should be addressed. E-mail: agp6@columbia.edu. Phone: (212) 305-8675. Fax: (212) 305-6949.

[1] Abbreviations: iGluR, ionotropic glutamate receptor; GluR2, ionotropic glutamate receptor subtype 2 or B; S1S2, ligand-binding domain sequences; AMPA, α-amino-3-hydroxy-5-methyl-4-isoxazole propionic acid; NMDA, *N*-methyl-D-aspartate.

10.1021/bi047984f CCC: $30.25
Published on Web 02/11/2005

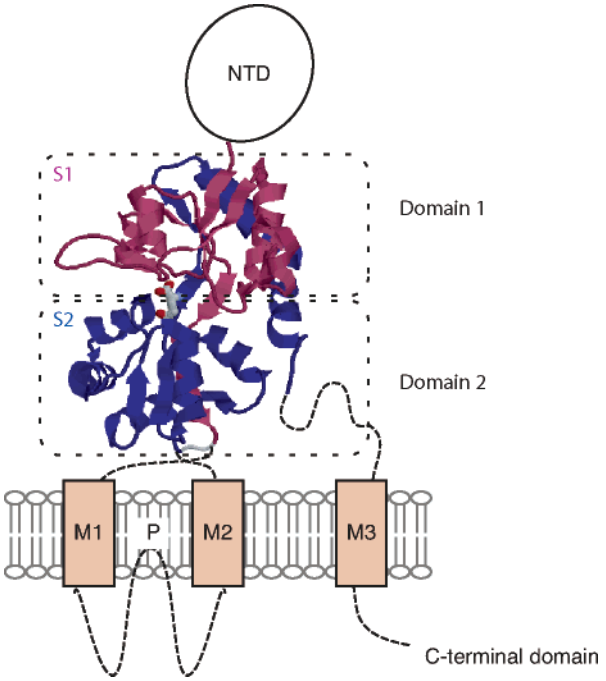

FIGURE 1: General topology of an iGluR protomer. Shown are the relative arrangements of the N-terminal domain (NTD), the S1S2 ligand-binding domain, three transmembrane helices (TM1−TM3), the re-entrant pore loop (P), and the C-terminal domain. A ribbon diagram of the crystal structure of the S1S2 domains is included. Portions for which there is no known structure are shown schematically or with dotted lines. (Adapted with permission from ref *11*.)

residues compared with glutamate and quisqualate. The α-constituents of each ligand interact in similar fashion with amino acid residues in the GluR2 S1S2 domain. In contrast, the γ-constituents of the ligands interact with different subsites in the GluR2 S1S2 domain (*15*). In addition, the trans peptide bond between Asp651 and Ser652 is observed in two different conformations in the X-ray crystal structures; this structural heterogeneity is called the "peptide flip" and is shown in Figure 3 (*4*, *15*). The flipped conformation is caused by a 180° change in ψ at Asp651, a 157° change in ϕ and an 80° change in ψ at Ser652, and a 64° change in ϕ at Gly653 with respect to the conformation in the unflipped state (*4*). In the flipped conformation, two additional hydrogen bonds form between domains 1 and 2: the carbonyl of Ser652 with the amide of Gly451 and the carbonyl of Asp651 with the amide of Tyr450 interact through an intermediary water molecule (*4*). The peptide flip conformation is observed in the crystal structures of AMPA-, glutamate-, and quisqualate-bound GluR2. However, in the AMPA-bound form, all three protomers in the asymmetric unit are in the flipped conformation, whereas in the glutamate bound form only one of the three protomers is in the flipped conformation (*4*). In the two crystal forms of quisqualate-bound S1S2, four of the five protomers are in the flipped conformation (*15*). This observation implies that the peptide flip represents a dynamic equilibrium, at least in glutamate- and quisqualate-bound GluR2 S1S2. Despite the structural differences in binding modes, AMPA and quisqualate bind to GluR2 S1S2J with approximately the same affinities, and glutamate binds with approximately 10-fold weaker affinity (*15*). Furthermore, the three agonists exhibit similar channel activation and desensitization kinetics in electrophysiological studies of intact receptors (*15*).

An investigation of conformational dynamics of glutamate-bound GluR2 S1S2 by ^{15}N NMR spin relaxation has been reported (*16*). This work identified motions on microsecond-to-millisecond (μs−ms) and picosecond-to-nanosecond (ps−ns) time scales that may have consequences for both ligand binding and coupling of ligand binding to channel opening. The main results outlined in this work are the following: the binding residues in contact with the α-substituents of glutamate (those in domain 1) are relatively rigid, whereas those residues in contact with the γ-substituents of glutamate are more flexible (in domain 2); the β-sheet core of domain 2 exhibits μs−ms motions; helix F is flexible and provides a possible escape route for ligand without domain opening; and movement along helix I is in agreement with the hinge region identified from X-ray crystal structures. These results imply that dynamics of the ligand-binding domain may be important to iGluR function.

Herein, to elucidate differences in protein structure and conformational dynamics caused by binding of different ligands, chemical shift perturbation and chemical exchange line broadening of backbone amide ^{15}N resonances are examined by NMR spectroscopy for the GluR2 S1S2J ligand-binding domain in the presence of three different agonists: glutamate, quisqualate, and AMPA. The results imply that differences exist between the three ligand−protein complexes in solution that are not observed in the X-ray crystal structures determined to date. Furthermore, the locations of residues exhibiting the most pronounced ligand-dependent changes in conformational dynamics suggest that subtle differences may exist in the effects of these agonists on GluR2 function.

EXPERIMENTAL PROCEDURES

Materials. Glutamic acid (Sigma), *S*-quisqualic acid, and *S*-AMPA (Tocris) were used without further purification. Ligands were dissolved to 10 mM in the buffer used for NMR spectroscopy (pH 5.0, 20 mM sodium acetate, 100 mM NaCl, 0.5 mM EDTA, 1 mM NaN_3, and 10% D_2O). The GluR2 S1S2J construct has been described previously (*4*).

Sample Preparation. Samples were prepared by refolding overexpressed S1S2J from inclusion bodies using the previously described protocol (*18*, *19*). Isotopically labeled samples were prepared by overexpression in M9 media with $^{15}NH_4Cl$, $^{13}C_6O_6H_{12}$ glucose, and ^2H_2O as appropriate. Samples used for sequential assignments were ^{2}H, ^{15}N, ^{13}C labeled, while samples used for spin relaxation measurements were ^{15}N and ^{2}H labeled. Samples were approximately 85% deuterated. Samples were purified using buffers containing 1 mM glutamate, dialyzed extensively against NMR buffer, and exchanged into NMR buffer containing 10 mM ligand. Samples containing quisqualate and AMPA were concentrated to 0.5 mM, and samples containing glutamate were concentrated to 0.35 mM.

NMR Experiments. All spectra were recorded using Bruker DRX600 (Columbia University), Avance600 (New York Structural Biology Center), or Avance800 (New York Structural Biology Center) NMR spectrometers. Spectra were recorded at 298 K, as calibrated using a 100% methanol sample. All spectra were processed using NMRPipe software (*20*) and analyzed with Sparky (*21*).

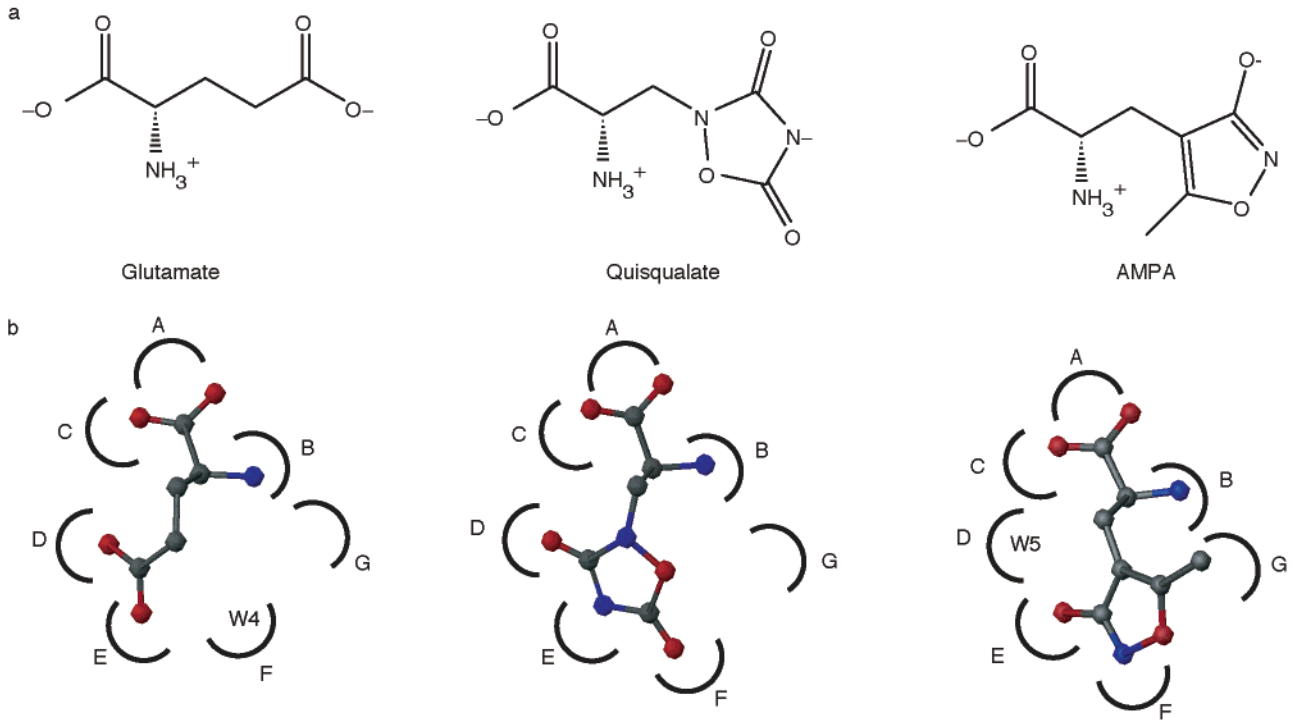

FIGURE 2: Schematic ligand-binding interactions in GluR2 S1S2. (a) Chemical structures of glutamate, quisqualate, and AMPA. (b) Binding modes of glutamate, quisqualate, and AMPA to GluR2 S1S2 as determined by X-ray crystallography (Adapted with permission from ref *15*.) Sites A−G represent the backbone and side-chain groups in GluR2 S1S2 that bind to the various ligands. Sites A, B, and C, occupied by Arg485, Thr480, and Ser654 respectively, bind equivalently to the α-substituents of all three ligands (*4*). Sites D, E, and F are occupied by Ser654 NH and Thr655 NH (site D), Thr655 OH (site E), and Glu705 NH (site F), respectively, and site G is occupied by side chains from Glu402, Tyr450, Pro478, Glu705, Met708, and Tyr732 (*4*). Met708 is in helix I. Both glutamate and quisqualate have ligand interactions with only sites A−F and do not occupy site G. Although glutamate does not directly interact with site F, a crystallographic water molecule, W4, occupies this site in the glutamate-bound structure. AMPA interacts with all sites A−G except for site D, which is occupied by a crystallographic water molecule, W5.

Sequential Assignments. Resonance assignments for glutamate-bound GluR2 S1S2 have been reported (*22*). Resonance assignments have been reported for an AMPA-bound GluR2 S1S2 construct that is 29 amino acids longer, a result of an N-terminal extension, at pH 7.0 and 303 K (*23*). These assignments were transferred to pH 5.0 by a series of HSQC spectra taken at pH 7.0, pH 6.3, and pH 5.0. The assignments for backbone resonances were confirmed using HNCA and HN(CO)CA spectra (*24*). Quisqualate-bound assignments were obtained by comparison to the glutamate-bound spectra and by use of HNCA, HN(CO)CA, HNCACB, and HN(CO)CACB spectra (*24*).

Chemical Shift Perturbation. For a pair of ligands, 1 and 2, the chemical shift perturbation, $\Delta\delta$, was determined using the following formula: $\Delta\delta = [(10\Delta\delta_H)^2 + \Delta\delta_N{}^2]^{1/2}$, in which $\Delta\delta_N = \delta_{N_2} - \delta_{N_1}$, $\Delta\delta_H = \delta_{H_2} - \delta_{H_1}$, and δ_{N_k} and δ_{H_k} are the chemical shifts for the ^{15}N and ^{1}H backbone amide spins for the complex between GluR2 S1S2 and the *k*th ligand, respectively.

NMR Relaxation Experiments. Transverse relaxation rate constants were measured with two different experiments, a WALTZ-16 ^{1}H-decoupled Hahn spin−echo pulse sequence (*25*, *26*) and a CPMG pulse sequence (*27*). The relaxation rate constants obtained from these two experiments are denoted $R_2{}^{HE}$ and $R_2{}^{CPMG}$, respectively. The relaxation delay for the Hahn spin−echo experiment was set to $\tau_{cp} = 58$ ms. Pulse field strengths were 25000 Hz for ^{1}H hard pulses, 1670 Hz for the ^{1}H WALTZ decoupling pulse, 6250 Hz for the ^{15}N hard pulses, and 1250 Hz for the ^{15}N Garp decoupling. The recycle delay was set to 3 s. Four pairs of spectra were recorded with $\tau_{cp} = 0$ ms and $\tau_{cp} = 58$ ms. $R_2{}^{HE}$ values for individual pairs of spectra were calculated assuming a monoexponential decay. Reported values of $R_2{}^{HE}$ are the averages of duplicate measurements, and reported uncertainties are taken to be the standard deviation of the duplicate measurements. For the CPMG experiment, the delay between the center of the π pulses on ^{15}N was set to be $\tau_{cp} = 1.0$ ms. The total CPMG relaxation delay was set at the following values: 0.004, 0.008, 0.014, 0.020, 0.028, 0.036, 0.044, 0.052, 0.060, and 0.068 s. The shortest and longest time points were taken in duplicate. Pulse field strengths were 25000 Hz for ^{1}H hard pulses, 6250 Hz for the ^{15}N hard pulses, including the 180° CPMG pulses, and 1250 Hz for the ^{15}N Garp decoupling. The recycle delay was set to 3 s. Relaxation rate constants $R_2{}^{CPMG}$ were calculated from peak intensity decays by fitting with CurveFit (www.columbia.hs.palmer.edu). Uncertainties were calculated using jack-knife simulations (*28*). In addition, the chemical exchange contribution to transverse relaxation, R_{ex}, was determined using a TROSY-based Hahn spin−echo experiment for mapping chemical exchange in large proteins (*26*). The spin−echo delay was 32 ms. Pulse field strengths were 25000 Hz for ^{1}H hard pulses and 6250 Hz for the ^{15}N hard pulses. The recycle delay was set to 2.5 s (glutamate measurements) and 3 s (quisqualate and AMPA measurements). Values of R_{ex} were calculated as described elsewhere (*26*).

Identifying Chemical Exchange. Chemical exchange line broadening results from μs−ms time scale conformational dynamics. Elevated R_2 values are indicative of chemical exchange based on the following equation: $R_2 = R_2{}^0 + R_{ex}$,

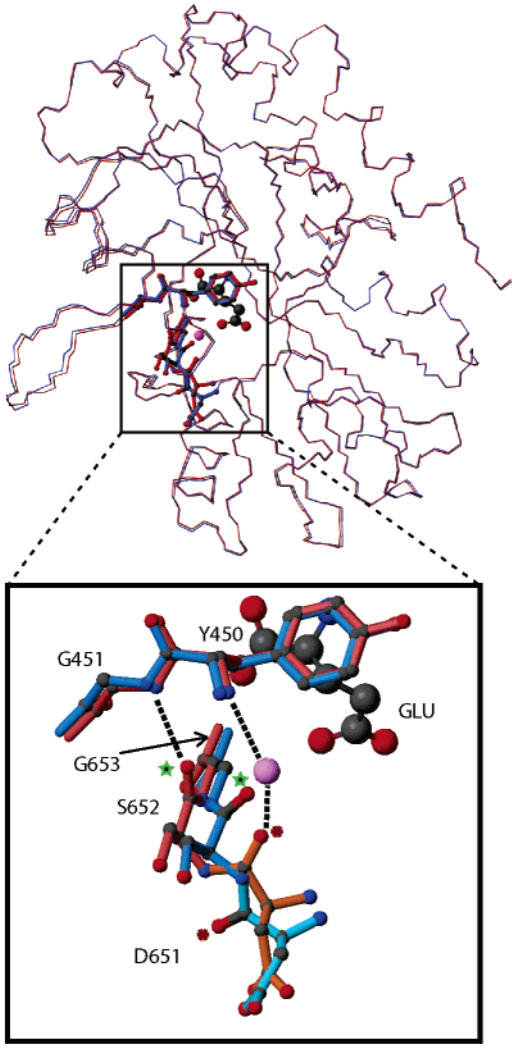

FIGURE 3: Conformations of the peptide flip in GluR2 S1S2. The AMPA- (red/orange, pdb 1ftm chain a) and glutamate-bound (blue/cyan, pdb 1ftj chain a) crystal structures are overlaid, and the peptide flip region is expanded for a closer view. The "peptide flip" is shown here in both the flipped (red/orange, AMPA-bound) and unflipped (blue/cyan, glutamate-bound chain a) conformations. The flipped conformation is caused by a 180° change in ψ at Asp651, a 157° change in ϕ and an 80° change in ψ at Ser652, and a 64° change in ϕ at Gly653 with respect to the conformation in the unflipped state (*4*). The green stars indicate the backbone carbonyl of Ser652, and the red asterisks indicate the backbone carbonyl of Asp651. The flipped conformation allows two additional hydrogen bonds between domains 1 and 2 (see Figure 1) mediated through the backbone carbonyls of Asp651 and Ser652 with the backbone amides of Tyr450 and Gly451, respectively. The hydrogen bond between Asp651 and Tyr450 is water mediated, and the water, present in the AMPA-bound crystal structure, is shown in purple. The bound conformation of glutamate is depicted as a ball-and-stick representation.

in which R_2^0 is the transverse relaxation rate constant in the absence of exchange. Chemical exchange can be detected directly from values of $R_{ex} > 0$ determined from the TROSY-based Hahn spin−echo experiment. Additional residues affected by chemical exchange processes were identified by comparing R_2^{HE} and R_2^{CPMG} relaxation rate constants. The CPMG experiment suppresses chemical exchange in which the value of $1/k_{ex}$ is on the order of $\tau_{CP} = 1$ ms or slower. In contrast, the Hahn spin−echo experiment suppresses chemical exchange only when the value of $1/k_{ex}$ is greater than the spacing between the Hahn echo pulse, $\tau_{HE} = 58$ ms. If

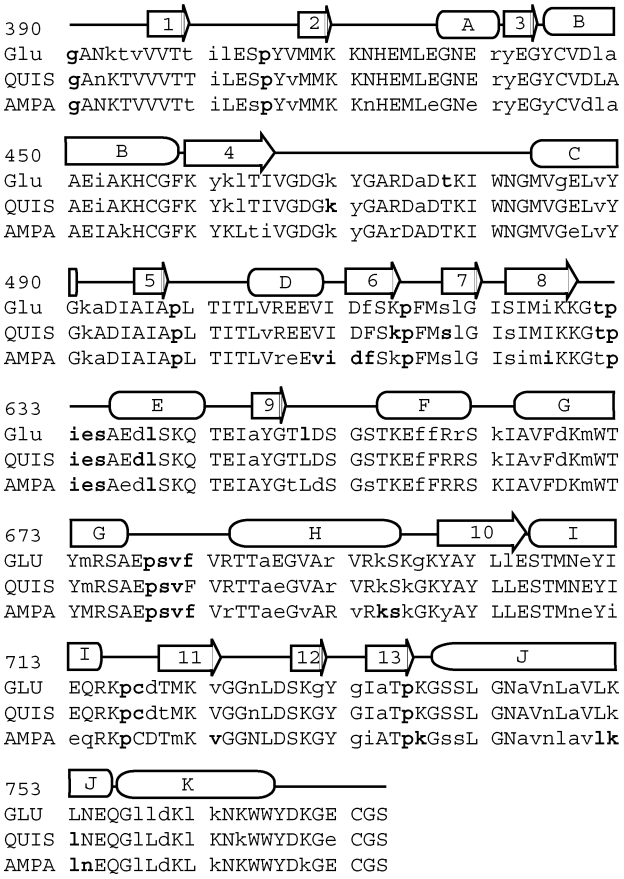

FIGURE 4: Resonance assignments in glutamate-, quisqualate-, and AMPA-bound GluR2 S1S2. Unassigned resonances are in boldface, lowercase type. Resonances that are not included in the relaxation analysis because they are unassigned or overlapped in the NMR spectra are shown in lowercase letters. The secondary structural elements of GluR2 S1S2 are indicated.

$R_2^{HE} > R_2^{CPMG}$, then the resonance is broadened by a chemical exchange process with a rate constant $1/k_{ex} \approx 1$ ms, because R_2^0 is equivalent in both experiments.

RESULTS

Sequential Assignments. Resonance assignments of backbone amide moieties for glutamate- (*22*), quisqualate-, and AMPA-bound GluR2 S1S2 at pH 5.0 and 298 K are 94%, 94%, and 89% complete. Residues that remain unassigned for the three different ligand-bound states are shown in bold and lowercase in Figure 4. The residues that are not assigned in the AMPA-bound complex, but are assigned in glutamate- or quisqualate-bound forms, are found in helix B, strand 6, helix H, and helix J. Interestingly, helix J is near the dimer−dimer interface of the protein and appears to have different spectral properties in AMPA-bound than in glutamate- and quisqualate-bound GluR2 S1S2.

Chemical Shift Perturbations. Chemical shift perturbations, $\Delta\delta$, were determined between the different ligand-bound complexes of GluR2 S1S2 and are shown in Figure 5b. Tentative assignments for helix J in the AMPA-bound complex, based on the assignments at pH 7.0, are used in this figure. Overall, the chemical shift differences are greater for AMPA-bound than for quisqualate-bound when either is compared to glutamate-bound GluR2 S1S2. The chemical shift perturbations between AMPA- and glutamate-bound

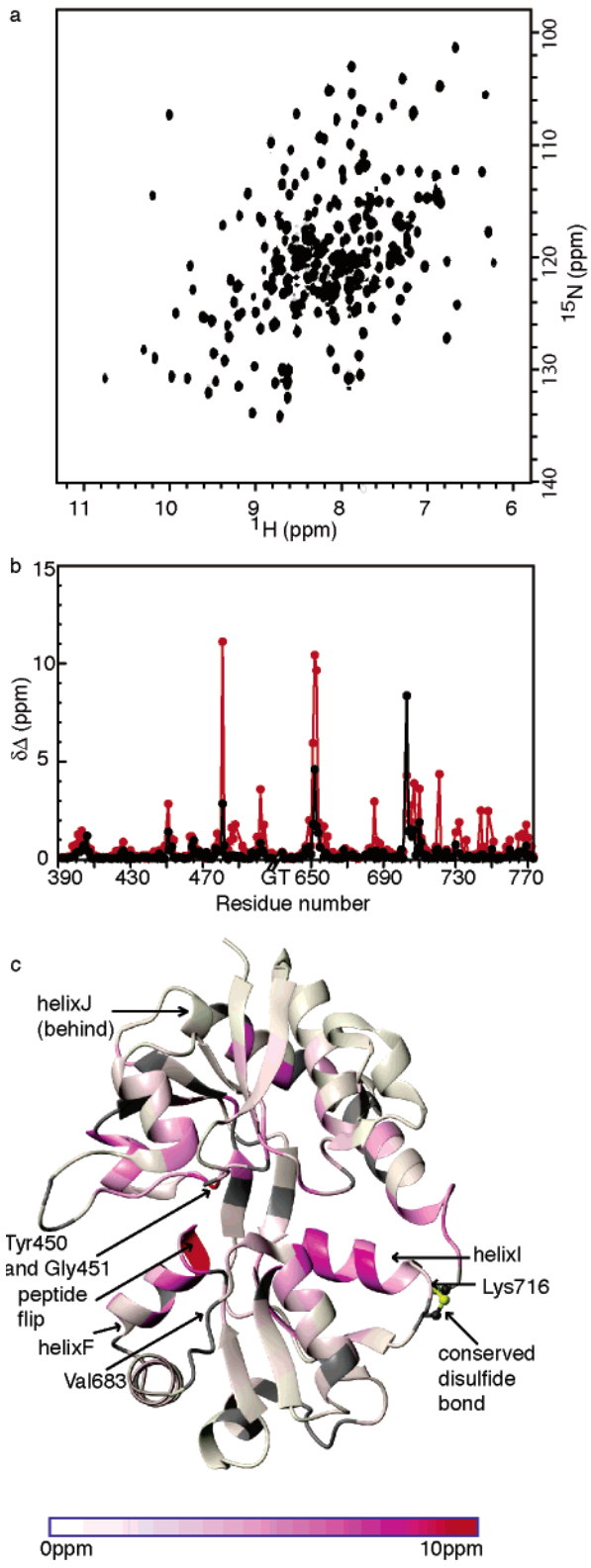

FIGURE 5: Chemical shift perturbations. (a) A ^{1}H ^{15}N TROSY correlation spectrum is shown for glutamate-bound GluR2 S1S2. (b) Chemical shift perturbations, $\Delta\delta$, are shown for AMPA- (red) and quisqualate-bound (black) GluR2 S1S2, compared to the glutamate-bound complex, as a function of the linear sequence of GluR2 S1S2. GT indicates the linker region between S1 and S2. (c) Chemical shift perturbations of AMPA-bound, compared to glutamate-bound, GluR2 S1S2 mapped onto a ribbon diagram of glutamate-bound GluR2 S1S2 (pdb 1ftj, protomer a). The peptide flip of GluR2 S1S2 is shown in the unflipped conformation.

GluR2 S1S2 are mapped onto the glutamate-bound crystal structure in Figure 5c. The three areas of large chemical shift changes are along helix I; around Asp651, Ser652, and helix F; and in helix J. These changes all are located in S2 and mostly in domain 2. More minor chemical shift changes occur in residues in S1 and domain 1.

Chemical Shift Perturbations May Identify the Peptide Flip. One interesting example of shift perturbation is provided by Tyr450 and Gly451. The side chain of Tyr450 is oriented nearly identically in the ligand-binding site in the crystal structures of the complexes of all three ligands. The changes in the backbone chemical shifts, therefore, are unlikely to be due to a different rearrangement of the side chains. However, Tyr450 can form a hydrogen bond with Asp651. This hydrogen bond forms only when the so-called "peptide flip" between Asp651 and Gly652 occurs. This flip is always observed in the AMPA-bound crystal structures, but multiple conformations are observed in both the quisqualate- and glutamate-bound crystal structures (*4*, *15*). Thus, the change in chemical shifts for Tyr450 may reflect averaging between the different peptide flip conformations. In further support of this idea, the chemical shifts of the Asp-Ser-Gly "peptide flip" region also are drastically different in AMPA-bound compared to glutamate-bound GluR2 S1S2. In fact, in quisqualate-bound GluR2, the chemical shifts of this region are nearly identical to those for glutamate-bound GluR2 S1S2, with the exception of Ser654, which is directly contacting ligand. Chemical shift differences in this region also may arise because of differences in the ligand atoms present in AMPA-bound GluR2 as compared with the glutamate- and quisqualate-bound structures (Figure 2).

Relaxation Data. R_2^{HE}, R_2^{CPMG}, and R_{ex} data were measured for glutamate-, quisqualate-, and AMPA-bound GluR2 S1S2J. Overlapped residues that could not be analyzed are shown in lowercase in Figure 4. A total of 78%, 78%, and 65% of the backbone ^{15}N resonances were analyzed for glutamate-, quisqualate-, and AMPA-bound GluR2 S1S2, respectively. The R_2^{HE} data are shown in Figure 6, and the R_{ex} data are shown in Figure 7. The R_2^{HE} and R_2^{CPMG} data are compared for quisqualate- and AMPA-bound GluR2 S1S2 in Figure 8.

Glutamate-Bound GluR2 S1S2 Has a Greater Tendency To Self-Associate Than AMPA- and Quisqualate-Bound GluR2 S1S2J. Transverse relaxation data recorded at 0.5 mM protein concentration showed that glutamate-bound GluR2 S1S2 has an average R_2 value that is about 2 s^{-1} greater than those for AMPA- and quisqualate-bound GluR2 S1S2 (not shown). Measurements recorded for glutamate-bound GluR2 S1S2 with a 0.35 mM protein concentration no longer exhibited increased values of R_2. For this reason, relaxation data are presented for glutamate-bound GluR2 S1S2 at 0.35 mM protein concentration and for AMPA- and quisqualate-bound GluR2 S1S2 at 0.5 mM protein concentration. Under these conditions, GluR2 S1S2 is greater than 98% monomeric (*17*). The CPMG experiment was not performed for glutamate-bound GluR2 S1S2 at 0.35 mM protein concentration.

Residues Undergoing Chemical Exchange. Significant exchange broadening is evident for Val 683 and Lys 716 in glutamate- and quisqualate-bound GluR2 S1S2, but the exchange broadening of these residues is reduced in AMPA-bound GluR2 S1S2. Cys718 exhibits chemical exchange broadening in AMPA-bound GluR2, but results are not

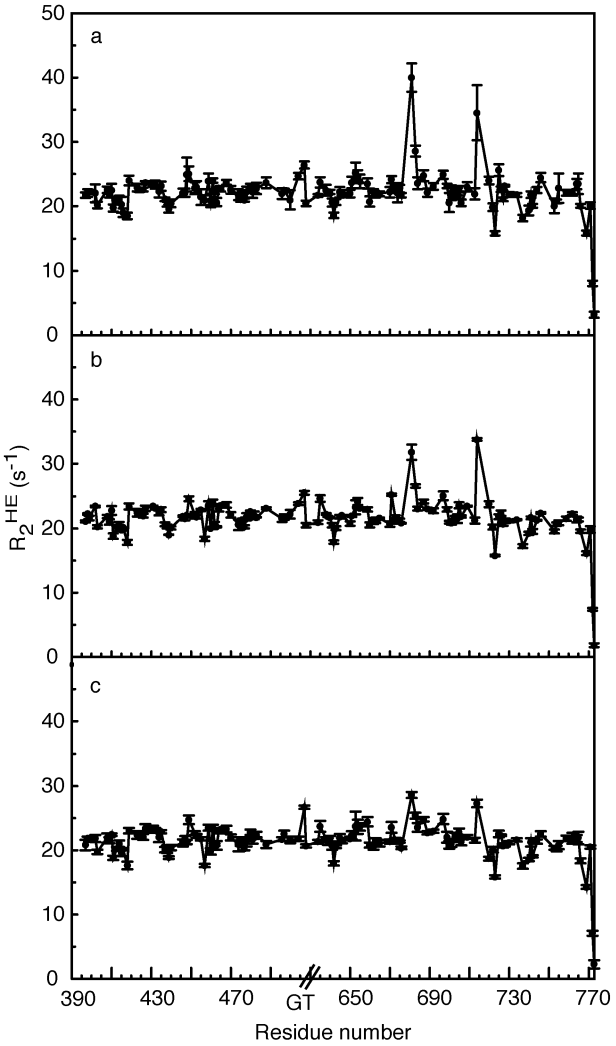

FIGURE 6: R_2^{HE} relaxation rate constants for (a) glutamate-, (b) quisqualate-, and (c) AMPA-bound GluR2 S1S2. Significantly elevated R_2 rate constants are observed at two sites of the protein, Val683 and Lys716. The R_2 rate constant for these two residues is reduced in AMPA-bound GluR2 S1S2.

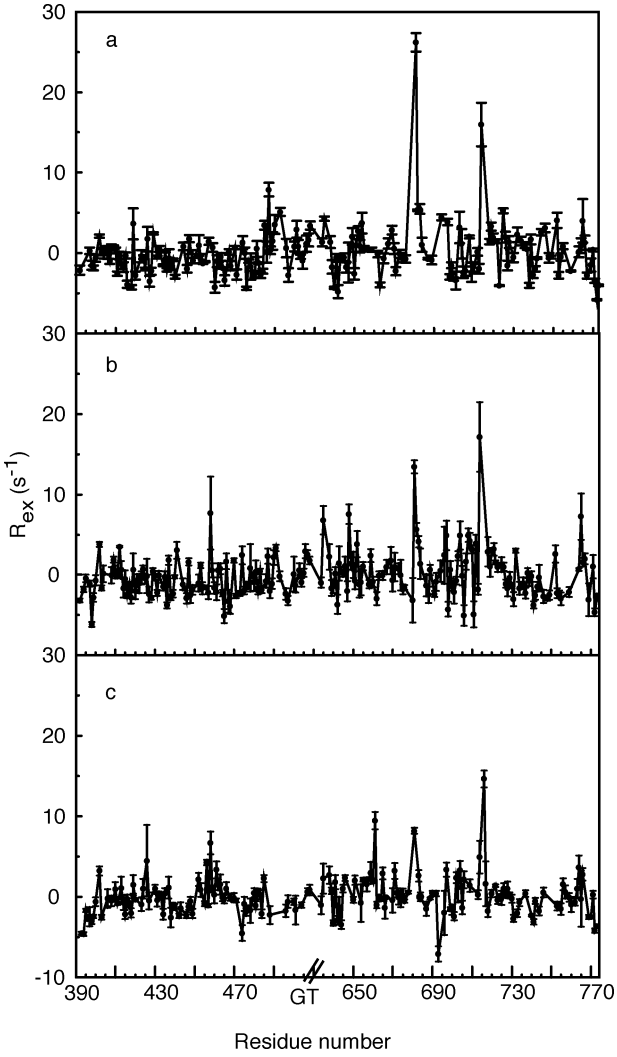

FIGURE 7: Chemical exchange, R_{ex}, in (a) glutamate-, (b) quisqualate-, and (c) AMPA-bound GluR2 S1S2. R_{ex} is greatest for residues Val683 and Lys716 in glutamate-bound GluR2 S1S2. Exchange at residue Lys716 is suppressed, and exchange for Cys718 is observed in AMPA-bound GluR2 S1S2 (c). Residue Cys718 is not assigned for (a) glutamate- or (b) quisqualate-bound GluR2 S1S2 and is possibly too exchange broadened to be detected.

available for the glutamate- and quisqualate-bound complexes because the residue is unassigned. In all likelihood, resonances for Cys718 are unassigned in these complexes because severe chemical exchange line broadening results in undetectable signal intensities. Thus, the region from Lys716 to Cys718 is likely sampling multiple conformations when any of the three agonists are bound to GluR2 S1S2, but broadening is reduced in the AMPA-bound complex because the rate constant of the conversion, k_{ex}, and the site populations depend on the bound agonist. When the R_2^{HE} and R_2^{CPMG} values are compared, quisqualate-bound GluR2 S1S2 displays more residues with exchange broadening than AMPA-bound GluR2 S1S2. In fact, for the AMPA-bound complex, only Thr457, Val683, and Gly698 have $R_2^{HE} > R_2^{CPMG} + 2.5\ s^{-1}$. Thr457, located in loop 2, also shows exchange broadening in the direct measurement of R_{ex} and is exchange broadened in all three ligand-bound states. Val683 is exchange broadened in all three cases, but the value of R_{ex} is different for the different ligands, implying a difference in populations or resonance frequencies of the exchanging sites and/or a change in the rate constant of exchange. Gly698 is located in a loop between helix H and strand 10. In quisqualate-bound GluR2, the residues for which $R_2^{HE} > 2.5 + R_2^{CPMG}$ include Lys409, Thr457, Trp460, Val488, Val683, Thr685, Val693, Gln714, and Lys716. Lys409 is located at the beginning of a loop between strand 2 and helix A. Thr457 and Trp460 are located in loop 1, and Val488 is located in the loop between helix D and strand 6. Val693 and Thr685 are located at the beginning of helix H, and Gln714 and Lys716 are located at the C-terminal end of helix I and next to the conserved disulfide bond. R_{ex} and R_2^{HE} results for glutamate- and quisqualate-bound GluR2 are similar, but R_2^{CPMG} was not measured at 0.35 mM glutamate-bound GluR2 S1S2. R_2^{CPMG} for a 0.5 mM sample was similar to that for quisqualate-bound GluR2, except for a uniform elevation of all rate constants, as discussed above (data not shown).

DISCUSSION AND CONCLUSION

To explore the effects of different agonist molecules on glutamate receptor function, conformational dynamic properties of GluR2 S1S2 domain complexed with three agonists—

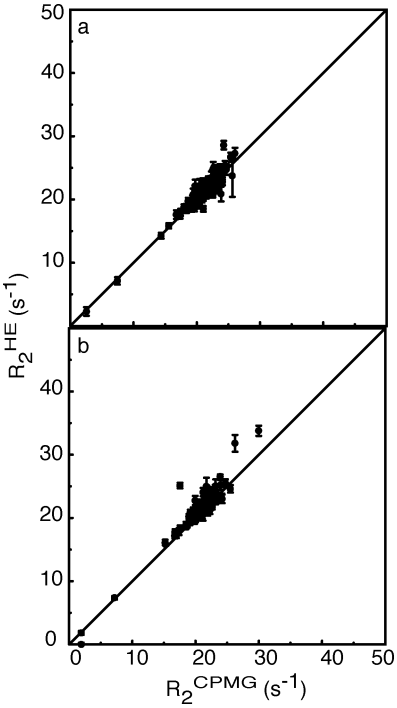

FIGURE 8: Comparison of R_2^{HE} and R_2^{CPMG} relaxation rate constants for (a) AMPA- and (b) quisqualate-bound GluR2 S1S2. Differences in R_2^{HE} and R_2^{CPMG} relaxation rate constants imply chemical exchange broadening on a time scale ≥1 ms. More extensive exchange broadening on this time scale is observed for quisqualate- than for AMPA-bound GluR2 S1S2.

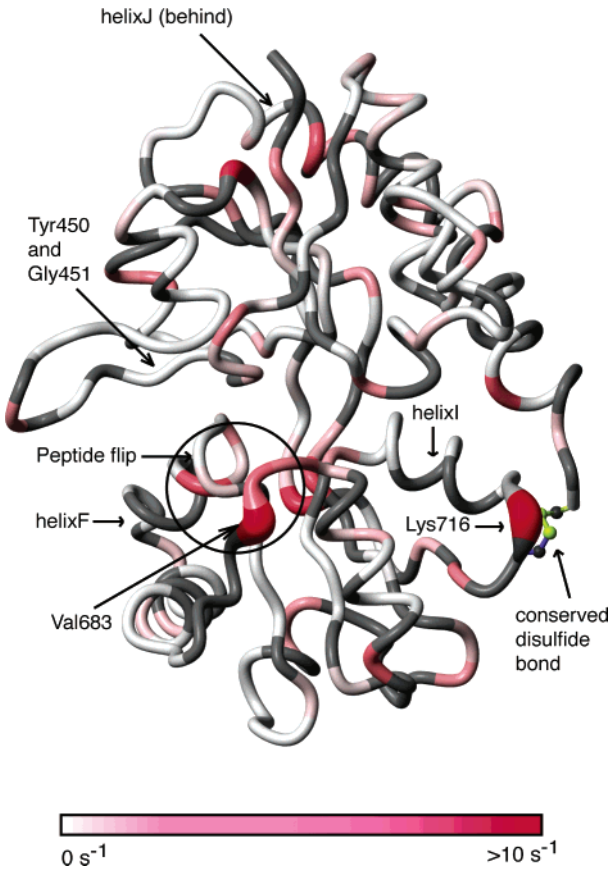

FIGURE 9: Difference in R_{ex} between glutamate- and AMPA-bound GluR2 S1S2 mapped onto the glutamate-bound GluR2 S1S2 structure (pdb 1ftj). Gray indicates amino acids that were not analyzed. Differences are color-coded from white, 0 s^{-1}, to red, ~10 s^{-1}. The potential subdomain between the loop containing Val683 and the peptide flip is circled.

glutamate, quisqualate, and AMPA—have been characterized by NMR spectroscopy. The chemical shift and chemical exchange differences between the different GluR2 S1S2 complexes imply that, in solution, AMPA-bound GluR2 S1S2 samples different conformations than glutamate- and quisqualate-bound GluR2 S1S2, despite the similarity of the crystal structures. GluR2 S1S2 binds quisqualate and AMPA with similar affinities, about 10-fold greater than the affinity for glutamate. If the effects observed by NMR were caused simply by differences in binding affinity, then the properties of the AMPA- and quisqualate-bound GluR2 S1S2 complexes would be more similar, instead of the trend that is observed. Thus, the experimental results are most likely attributable to the different binding modes of the three ligands, as opposed to differences in binding affinity.

Two areas of the protein show the greatest differences in both chemical exchange line broadening and chemical shift perturbation for AMPA-bound GluR2 S1S2, when compared to glutamate- and quisqualate-bound GluR2 S1S2: the region surrounding Val683 and the region around the disulfide bond, Lys716-Cys718. Val683 occurs in a loop between helix G and helix H and is in a potential subdomain that also includes the Asp-Ser-Gly peptide flip segment. These two loops are proximal in three-dimensional space and may be involved in correlated motional processes (Figure 9). Crystal structures have demonstrated that the Asp-Ser-Gly region adopts multiple conformations in the glutamate- and quisqualate-bound states (*4*, *15*). Chemical shift perturbations also identify differences in the conformation of the Asp-Ser-Gly region in AMPA-bound GluR2 S1S2 when compared to glutamate- or quisqualate-bound GluR2 S1S2.

The area around the conserved disulfide bond in S1S2 also undergoes conformational exchange in the μs−ms time scale. This region undergoes exchange in all three liganded states studied here but exhibits markedly less chemical exchange line broadening in AMPA-bound GluR2 than in glutamate- and quisqualate-bound GluR2 S1S2. Lys716, which is present at the C-terminal end of helix I, is present in a loop and is two residues before Cys718, which is involved in a conserved disulfide bond in all iGluR's. Cys718 is not assigned in glutamate- or quisqualate-bound GluR2 and is mostly likely severely exchange broadened. In AMPA-bound GluR2 S1S2, Lys716 does not exhibit chemical exchange broadening but Cys718 does. Residue 717 is a proline and cannot be observed in $^1H-^{15}N$ correlation experiments. The chemical shifts of helix I are different in AMPA-bound GluR2 as well. Put together, these results imply that a difference in conformational dynamics for the area around helix I exists in the AMPA-bound state. Mutation of the cysteines in the disulfide bond has been shown in other studies to increase agonist affinity (*29*). Also, redox potentiation of NMDA receptors may occur in vivo (*30*). Thus, differences in dynamics of this region may affect the gating of the full-length receptor. Most significantly, changes in how the ligand interacts in the binding site appear to cause changes in dynamics of distal portions of the ligand-binding domain.

In conclusion, glutamate-, quisqualate-, and AMPA-bound GluR2 S1S2 ligand-binding domains have been investigated in solution by ^{15}N NMR spectroscopy to ascertain how the binding modes of agonist ligands affect equilibrium confor-

mations and μs−ms dynamical properties of the receptor. Changes in conformation and dynamics associated with changes in the ligand-binding mode, but not affinity, of glutamate, quisqualate, and AMPA couple the active site and distal membrane−proximal regions of the receptor. These results suggest subtle differences in the activities of the different agonist ligands toward ionotropic glutamate receptors.

ACKNOWLEDGMENT

We thank Ming-Ming Zhou and Lei Zeng (Mount Sinai) for the AMPA-bound GluR2 S1S2 resonance assignments at pH 7.0. We thank J. Eric Gouaux for assistance in preparing GluR2 S1S2 and for helpful discussions.

REFERENCES

1. Dingledine, R., Borges, K., Bowie, D., and Traynelis, S. F. (1999) The glutamate receptor ion channels, *Pharmacol. Rev. 51*, 7−61.
2. Mayer, M. L., Olson, R., and Gouaux, E. (2001) Mechanisms for ligand binding to GluR0 ion channels: crystal structures of the glutamate and serine complexes and a closed apo state, *J. Mol. Biol. 311*, 815−36.
3. Rosenmund, C., Stern-Bach, Y., and Stevens, C. F. (1998) The tetrameric structure of a glutamate receptor channel, *Science 280*, 1596−9.
4. Armstrong, N., and Gouaux, E. (2000) Mechanisms for activation and antagonism of an AMPA-sensitive glutamate receptor: crystal structures of the GluR2 ligand binding core, *Neuron 28*, 165−81.
5. Robert, A., Irizarry, S. N., Hughes, T. E., and Howe, J. R. (2001) Subunit interactions and AMPA receptor desensitization, *J. Neurosci. 21*, 5574−86.
6. Ayalon, G., and Stern-Bach, Y. (2001) Functional assembly of AMPA and kainate receptors is mediated by several discrete protein−protein interactions, *Neuron 31*, 103−13.
7. Madden, D. R. (2002) The structure and function of glutamate receptor ion channels, *Nat. Rev. Neurosci. 3*, 91−101.
8. Kuusinen, A., Arvola, M., and Keinanen, K. (1995) Molecular dissection of the agonist binding site of an AMPA receptor, *Embo J. 14*, 6327−32.
9. Arvola, M., and Keinanen, K. (1996) Characterization of the ligand-binding domains of glutamate receptor (GluR)-B and GluR-D subunits expressed in Escherichia coli as periplasmic proteins, *J. Biol. Chem. 271*, 15527−32.
10. Armstrong, N., Mayer, M., and Gouaux, E. (2003) Tuning activation of the AMPA-sensitive GluR2 ion channel by genetic adjustment of agonist-induced conformational changes, *Proc. Natl. Acad. Sci. U.S.A. 100*, 5736−41.
11. Armstrong, N., Sun, Y., Chen, G. Q., and Gouaux, E. (1998) Structure of a glutamate-receptor ligand-binding core in complex with kainate, *Nature 395*, 913−7.
12. Hogner, A., Greenwood, J. R., Liljefors, T., Lunn, M. L., Egebjerg, J., Larsen, I. K., Gouaux, E., and Kastrup, J. S. (2003) Competitive antagonism of AMPA receptors by ligands of different classes: crystal structure of ATPO bound to the GluR2 ligand-binding core, in comparison with DNQX, *J. Med. Chem. 46*, 214−21.
13. Hogner, A., Kastrup, J. S., Jin, R., Liljefors, T., Mayer, M. L., Egebjerg, J., Larsen, I. K., and Gouaux, E. (2002) Structural basis for AMPA receptor activation and ligand selectivity: crystal structures of five agonist complexes with the GluR2 ligand-binding core, *J. Mol. Biol. 322*, 93−109.
14. Jin, R., and Gouaux, E. (2003) Probing the function, conformational plasticity, and dimer-dimer contacts of the GluR2 ligand-binding core: studies of 5-substituted willardiines and GluR2 S1S2 in the crystal, *Biochemistry 42*, 5201−13.
15. Jin, R., Horning, M., Mayer, M. L., and Gouaux, E. (2002) Mechanism of activation and selectivity in a ligand-gated ion channel: structural and functional studies of GluR2 and quisqualate, *Biochemistry 41*, 15635−43.
16. McFeeters, R. L., and Oswald, R. E. (2002) Structural mobility of the extracellular ligand-binding core of an ionotropic glutamate receptor. Analysis of NMR relaxation dynamics, *Biochemistry 41*, 10472−81.
17. Sun, Y., Olson, R., Horning, M., Armstrong, N., Mayer, M., and Gouaux, E. (2002) Mechanism of glutamate receptor desensitization, *Nature 417*, 245−53.
18. Chen, G. Q., Sun, Y., Jin, R., and Gouaux, E. (1998) Probing the ligand binding domain of the GluR2 receptor by proteolysis and deletion mutagenesis defines domain boundaries and yields a crystallizable construct, *Protein Sci. 7*, 2623−30.
19. Chen, G. Q., and Gouaux, E. (1997) Overexpression of a glutamate receptor (GluR2) ligand binding domain in Escherichia coli: application of a novel protein folding screen, *Proc. Natl. Acad. Sci. U.S.A. 94*, 13431−6.
20. Delaglio, F., Grzesiek, S., Vuister, G. W., Zhu, G., Pfeifer, J., and Bax, A. (1995) NMRPipe: a multidimensional spectral processing system based on UNIX pipes, *J. Biomol. NMR 6*, 277−93.
21. Goddard, T. D., and Kneller, D. G., Sparky 3, University of California, San Francisco, 2002.
22. McFeeters, R. L., Swapna, G. V., Montelione, G. T., and Oswald, R. E. (2002) Semi-automated backbone resonance assignments of the extracellular ligand-binding domain of an ionotropic glutamate receptor, *J. Biomol. NMR 22*, 297−8.
23. Zeng, L., Chen, C. H., Muller, M., and Zhou, M. M. (2003) Structure-based rational design of chemical ligands for AMPA-subtype glutamate receptors, *J. Mol. Neurosci. 20*, 345−8.
24. Cavanagh, J., Fairbrother, W. J., Palmer, A. G. I., and Skelton, N. J. (1996) *Protein NMR spectroscopy: principles and practice*, Academic Press, San Diego.
25. Wang, C. Y., Grey, M. J., and Palmer, A. G. (2001) CPMG sequences with enhanced sensitivity to chemical exchange, *J. Biomol. NMR 21*, 361−6.
26. Wang, C. Y., Rance, M., and Palmer, A. G. (2003) Mapping chemical exchange in proteins with MW > 50 kD, *J. Am. Chem. Soc. 125*, 8968−9.
27. Farrow, N. A., Muhandiram, R., Singer, A. U., Pascal, S. M., Kay, C. M., Gish, G., Shoelson, S. E., Pawson, T., Forman-Kay, J. D., and Kay, L. E. (1994) Backbone dynamics of a free and phosphopeptide-complexed Src homology 2 domain studied by 15N NMR relaxation, *Biochemistry 33*, 5984−6003.
28. Mosteller, F., and Tukey, J. W. (1977) *Data analysis and regression: a second course in statistics*, Addison-Wesley Pub. Co., Reading, MA.
29. Abele, R., Lampinen, M., Keinanen, K., and Madden, D. R. (1998) Disulfide bonding and cysteine accessibility in the alpha-amino-3-hydroxy-5-methylisoxazole-4-propionic acid receptor subunit GluRD. Implications for redox modulation of glutamate receptors, *J. Biol. Chem. 273*, 25132−8.
30. Choi, Y. B., and Lipton, S. A. (2000) Redox modulation of the NMDA receptor, *Cell Mol. Life Sci. 57*, 1535−41.

BI047984F